# = ATOMS, MOLECULES, OPTICS =

# SUPPRESSION OF LIGHT SHIFT OF COHERENT POPULATION TRAPPING RESONANCES IN CESIUM VAPOR USING DOUBLE FREQUENCY AND AMPLITUDE MODULATION OF LASER RADIATION

© 2024 V. I. Vishnyakov\*, D. V. Brazhnikov, and M. N. Skvortsov

Institute of Laser Physics Siberian Branch of the Russian Academy of Sciences, Novosibirsk, 630090 Russia \*e-mail: vladislav.vishnyakov@gmail.com

Received April 21, 2024 Revised April 21, 2024 Accepted May 06, 2024

**Abstract**. The light (ac Stark) shift of coherent population trapping (CPT) resonances in cesium vapor is studied under excitation by radiation from a vertical-cavity surface-emitting laser, whose current is modulated at a microwave frequency ( $\approx 4.6$  GHz). This approach is used in some state-of-the-art microwave quantum frequency standards (QFS). One of the main factors leading to degradation of long-term frequency stability of QFS is associated with the light shift of the CPT resonance due to variations in optical power P in the vapor cell. In this work, it is shown that using an additional electro-optic modulator assembled as a Mach-Zehnder interferometer makes it possible to effectively control the amplitudes of sidebands in the radiation spectrum. This allows finding such an optimal optical power value near which the resonance shift is insensitive to its small changes. The results are of interest for the development of CPT-based QFS.

The article is presented as part of the conference proceedings "Physics of Ultracold Atoms" (PUCA-2023), Novosibirsk, December 2023.

**DOI:** 10.31857/S004445102410e110

#### 1. INTRODUCTION

Compact quantum frequency standards (QFS) and atomic clocks based on them have already found a number of important applications in satellite navigation systems [1, 2], including deep space navigation systems [3], broadband communication networks [4], remote sensing systems [5, 6] and other applications. Currently, three main directions are actively developing in the creation of compact QFS, which use CPT resonance [7–9], double radiooptical resonance [1, 10] or various sub-Doppler resonances [11–18] observed in cells with cesium or rubidium vapor (see review [4]) as a frequency reference. The first two types of QFS operate in the microwave range, where the frequency equal to several GHz is stabilized. In the third case, the optical range frequency (hundreds of THz)

is stabilized, and then the frequency stability is transferred to the microwave range using optical microresonators [11]. The most compact are QFS based on CPT resonances, which also feature low power consumption (~1 W or less), which is especially important for mobile applications, including various space technologies using "nanosatellites" [3, 6].

A key element of CPT-based QFS (QFS/CPT) is a vertical-cavity surface-emitting laser (VCSEL) [7]. The design of this laser allows efficient modulation of the pump current at ultra-high frequencies (from units to tens of GHz) to obtain sidebands in its emission spectrum necessary for observing CPT resonances in cells filled with alkali metal vapor (usually Rb or Cs). VCSELs have a very low generation threshold current (~1 mA), which means that their power consumption is low.

The most important characteristic of any OFS is the residual frequency instability over long averaging time intervals ( $\tau \gtrsim 10^4$  s), characterized by Allan deviation  $(\sigma_v)$  [19]. In the case of QFS/CPT, significant contributions to long-term frequency instability come from the drift of total optical power in the vapor cell, as well as the drift of the microwave generator power, which changes the intensity ratios of various sidebands in the VCSEL emission spectrum. Both types of drift lead to a shift in the error signal formed from the CPT resonance by the lock-in amplifier within the QFS. This shift occurs mainly due to the ac Stark effect (light shift) for the energy levels of the clock transition  $|F_{g1}, m_{g1}|$ =0 $\rangle$   $\rightarrow$  |  $F_{g2}$ ,  $m_{g2}$ =0 $\rangle$  ("0-0" transition). Here  $F_{g1,g2}$ are the total angular momenta of hyperfine energy levels of the alkali atom's ground state, and the quantum numbers  $m_{g1,g2}$  describe the projections of these angular momenta on the quantization z.

The dependence of the light shift  $\Delta_f$  resonance on the frequency modulation index of VCSEL current, more precisely on the microwave modulation power  $(P_{\parallel})$ , usually has a nonlinear form, which may contain extrema, as well as intersections with the abscissa axis where the light shift equals zero [20, 21]. Such behavior of the function  $\Delta_f(P_{\mathfrak{u}})$  suggests an obvious way to suppress the influence of light shift on the resonance CPT and ultimately on the longterm stability of OFS. Specifically, depending on which parameter variations contribute more to frequency instability (variations in optical power P or variations in microwave power  $P_{ii}$ , it becomes possible to select an optimal frequency modulation index at which either variations P [22], or variations  $P_{\mu}$  [9] do not lead to a significant shift in the error signal.

In some special cases, for example, at a certain buffer gas pressure [23] or when choosing an optimal scheme for exciting K $\Pi$ H [24], CPT resonances [24], it becomes possible to simultaneously suppress the influence of small variations of both P, and  $P_{\mu}$  on the error signal shift. It is also possible to select such a VCSEL sample where at the same  $P_{\mu}$  the light shift will be smaller than for another VCSEL sample from the same manufacturer [25]. However, this approach does not allow controlling the light shift of the CPT resonance when using a specific VCSEL sample and appears to be non-universal and impractical for implementation in atomic clocks. Furthermore,

some VCSEL samples may not demonstrate the required nonlinear dependence  $\Delta_f(P_\mu)$ , at all, since when  $P_\mu$  increases, such VCSELs exhibit a multimode regime of laser generation [26].

Currently, various scientific groups continue to search for new methods to control and suppress the light shift in OFS/CPT. Most of them use pulse techniques where various laser radiation parameters are changed abruptly using external electro-optic and/or acousto-optic modulators (see, for example, [27–31]). The behavior of the light shift can also be controlled by changing the relative intensities of the sidebands in the emission spectrum, for example, using vapor temperature [32] or using double frequency modulation of the VCSEL pump current at microwave [33] or lower [34] frequencies. Note that when using conventional microwave modulation of VCSEL current, its emission spectrum, in general, does not correspond to the symmetrical spectrum that should be observed during frequency modulation. On the contrary, the sidebands of equal absolute orders, for example, orders +1 and -1, may not be equal in intensity. This spectrum asymmetry is often associated with the influence of parasitic amplitude modulation [35–37]. However, a more rigorous analysis of this problem reveals a strong influence of nonlinear intermode effects in VCSEL on the output radiation spectrum [38].

In our work, we investigate a new method of exciting CPT resonances, involving both modulation of the VCSEL pump current at a microwave frequency and subsequent amplitude modulation of laser radiation at the same frequency using an external electro-optic modulator (EOM). As an EOM, we use a modulator assembled according to the Mach-Zehnder interferometer type. Unlike the parasitic amplitude modulation in VCSEL, in our case this type of modulation is well controlled. Thus, there are more possibilities for controlling the laser field spectrum. In particular, this leads to a strongly nonlinear dependence of the error signal frequency shift on the total optical power, whereas when using only microwave modulation of the laser pump current, this dependence is close to linear (see also [20, 39, 40]). The nonlinear nature of the dependence  $\Delta_f(P)$  with the presence of an extremum allows using the optimal optical power  $P_{ont}$ , at which suppression of fluctuations and small drifts P on the frequency stability of QFS/CPT can be expected. It should also be noted that the

combination of "VCSEL + EOM" has not been previously used for spectroscopy of alkali metal atoms, which is also of interest.

#### 2. EXPERIMENT

The experimental setup scheme is shown in Fig. 1. It uses a commercially available VCSEL with a generation spectrum width of about 50 MHz and maximum optical power of about 250 µW. The laser power supply was implemented using a Bias Tee scheme, which allows mixing the DC power supply of the laser with a signal at a frequency of about 4.6 GHz from a microwave generator. In the experiment with double frequency and amplitude modulation, the signal from the generator was fed simultaneously to the laser and EOM (iXblue NIR-MX950-LN-20) using a splitter. The length of wires from the splitter to the laser and EOM could be different. Thus, it was possible to adjust the phase between amplitude and frequency types of modulation, equal to  $\varphi_1 - \varphi_2$ , shown in Fig. 1. Laser thermal stabilization was maintained with an accuracy of about 1 mK.

The VCSEL radiation passed through two optical isolators, shown in Fig. 1 as a single element. A half-wave plate  $(\lambda/2)$  allowed matching the linear polarization of radiation with the optical axis of the EOM fiber. After the EOM, part of the radiation was directed to a scanning Fabry-Perot interferometer (SA210-8B by Thorlabs) to study the spectral composition of radiation, having a free spectral

range of 10 GHz and transmission peak width of about 10 MHz. After a quarter-wave plate ( $\lambda$  / 4), another part of the radiation acquired circular polarization and was directed to a cell containing cesium vapor and buffer gas (neon, about 130 Torr). The cell was made of borosilicate glass and had a cubic shape with an edge length of about 5 mm and a small stem containing metallic cesium. The cell temperature was maintained constant at about 60°C using heating elements and a thermal stabilization system. This temperature was chosen so that the CPT resonance had sufficient contrast for measurements in the desired range of P and  $P_{u}$ values. Cell heating did not noticeably affect either the CPT resonance contrast or the error signal position. The diameter  $(1/e^2)$  of the laser beam in the cell was approximately 1 mm.

A three-layer magnetic shield made of permalloy was used to isolate the cell from external magnetic fields. The residual magnetic field in the center of the shield did not exceed  $100~\mu G$ . A solenoid located inside the shields was used to create a constant uniform magnetic field in the cell. This field allows removing the degeneracy of hyperfine energy levels of the atom's ground state for selective excitation of the "0–0" clock transition.

Multi-frequency laser radiation excited optical transitions in the  $D_1$ -line ( $\lambda \approx 895$  nm). The buffer gas led to significant collisional broadening of the absorption line, so the hyperfine splitting of the energy level in the excited state of cesium was not

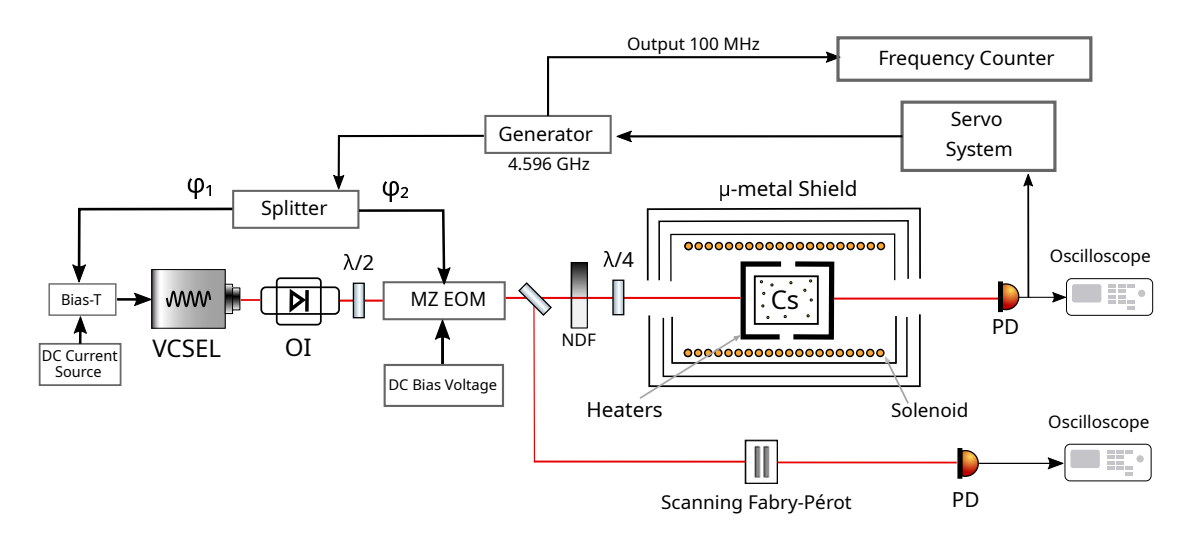


Fig. 1. Experimental setup scheme for observing CPT resonances using double frequency and amplitude modulation of laser radiation: VCSEL — vertical-cavity surface-emitting laser, OI — two Faraday optical isolators placed in series, MZ EOM — fiber electro-optical modulator assembled according to the Mach-Zehnder interferometer scheme, NDF — set of neutral filters,  $\lambda$  / 2,  $\lambda$  / 4 — wave plates, PD — photodetector

spectrally resolved. The VCSEL radiation frequency was stabilized to the center of the total absorption profile.

To form an error signal from the CPT resonance, the frequency lock-in system used a method similar to the Pound-Drever-Hall (PDH) method, widely studied for stabilizing the optical frequency of laser radiation using a high-Q cavity [41]. This method is currently actively used for QFS/CPT [9,42-44]. When using the PDH method to form an error signal, the CPT resonance is scanned at a frequency significantly exceeding its linewidth. In our case, this frequency was approximately 10 kHz with a resonance's half-width at half-maximum (HWHM) of about 1 kHz.

An example of CPT resonance is shown in Fig. 2a, which presents the central CPT resonance and two

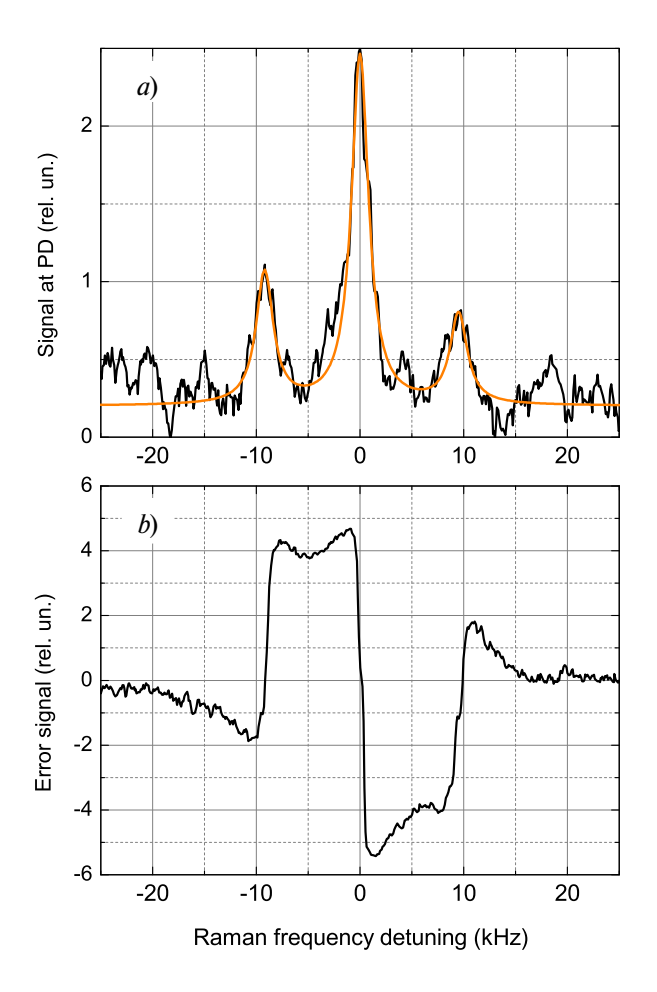
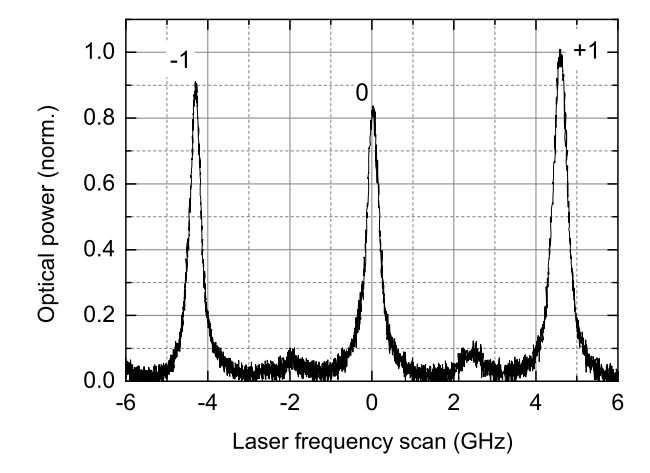


Fig. 2. a- CPT resonance excited by VCSEL radiation when modulating its pump current at a frequency of approximately 4.6 GHz. There is also a low-frequency current modulation at a frequency of about 10 kHz when using PDH regime The orange curve shows the approximation by three Lorentzian profiles, each with a half-width of about 1 kHz. b- Error signal at the output of the lock-in amplifier.  $P\approx20~\mu\text{W}, P_{\text{H}}\approx500~\mu\text{W}, T\approx60^{\circ}\text{C}$ 

side resonances, spaced approximately 10 kHz apart. The small difference in the amplitudes of the left and right peaks is mainly explained by noise influence, which was approximately 10% of the central peak for this resonance recording. The axis x shows the Raman (two-photon) frequency detuning:  $\delta_R = 2f_\mu - \delta_{hfs}$ , where  $f_\mu$  is the microwave generator frequency,  $\delta_{hfs}$  is the ground-state hyperfine splitting frequency in the atom of cesium (≈9.2 GHz). The shown CPT resonance is in the power broadening regime. The minimum resonance linewidth (at P  $\rightarrow 0$ ) is determined by the ground state relaxation rate in the cesium atom, which in our experiments is approximately 250 Hz. This value coincides with the calculated value based on data for diffusion coefficient and collision cross-sections from [45, 46]. The relaxation in the ground state of the atom is associated with the diffusive transit of the cesium atom through the light beam, with the spin exchange process between cesium atoms, and with depolarization due to collisions of cesium atoms with buffer gas atoms. The corresponding error signal is shown in Fig. 2b.

The process of measuring the light shift was as follows. The frequency lock-in electronics stabilized the microwave generator frequency at the CPT resonance using the PDH method described above. This frequency is related to the internal quartz oscillator frequency of 100 MHz through a specified division coefficient. Thus, the frequency stability from the microwave range is transferred to the radio range. Then, the 100 MHz signal frequency from the microwave generator output was compared using a VCH-323 comparator with the reference signal frequency from the CH1-1007 hydrogen frequency standard (JSC "Vremya-Ch"). Both devices are marked in Fig. 1 as Frequency Counter. The optical radiation power was changed in front of the cell every minute by replacing the neutral filter, which led to a corresponding frequency shift of 100 MHz at the output of the microwave generator. Thus, the comparator screen displayed a characteristic step function reflecting the frequency dependence on time.

An example of the radiation spectrum during current modulation of the VCSEL at a frequency of about 4.6 GHz is shown in Fig. 3. The observed large peaks, separated from each other by the microwave modulation frequency, represent the carrier frequency (0) and sidebands of orders -1



**Fig. 3.** VCSEL radiation spectrum with current modulated at 4.6 Ghz frequency. Numbers indicate the sideband order. The spectrum is normalized to the optical power of the spectrum sideband of order +1.  $P_{\rm u} \approx 500~\mu W$  ( $-3~{\rm dBm}$ )

and +1. Other peaks, slightly standing out against the noise background, are auxiliary modes of the interferometer, different from  $\mathrm{TEM}_{00}$ . The presented spectrum recording shows a small asymmetry: the optical power of the +1 order sideband exceeds the power of the -1 order sideband by approximately 10%. This asymmetry, together with the non-zero single-photon detuning from optical transitions in the  $D_1$ -line, can lead to asymmetry of the CPT resonance [47] and corresponding effective zero shift of the error signal. We assume that this effect is responsible for the nonlinear dependence observed in our experiments  $\Delta_f(P)$ , since its qualitative behavior agrees with the theory developed in work [44] based on a simplified  $\Lambda$ -scheme of the atom.

The influence of VCSEL spectrum asymmetry on the error signal shift depends not only on the difference in optical powers of the corresponding sidebands but also on the total optical power [44]. Meanwhile, the relatively small asymmetry of the VCSEL spectrum does not significantly affect the linear nature of the error signal shift dependence of the total optical power, which is reflected in Fig. 4a (see also [20, 39, 40]). This figure shows data for the light shift without the constant component, which is mainly related to the buffer gas influence — collisional shift (approximately 80 kHz according to [48]).

In our case, the spectrum asymmetry magnitude can be controlled not only by the power of the microwave generator signal but also by changing

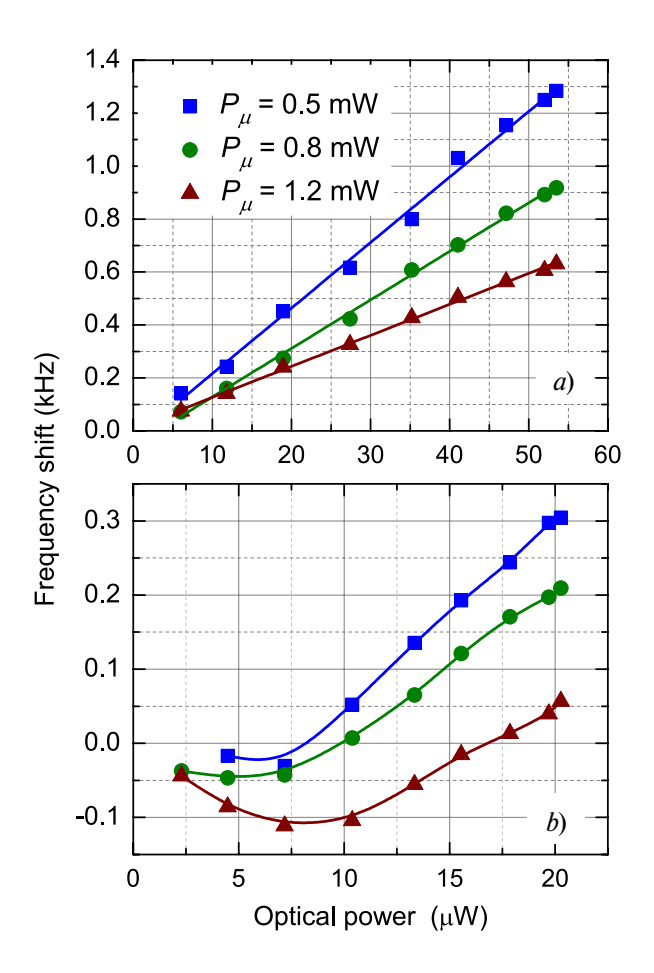
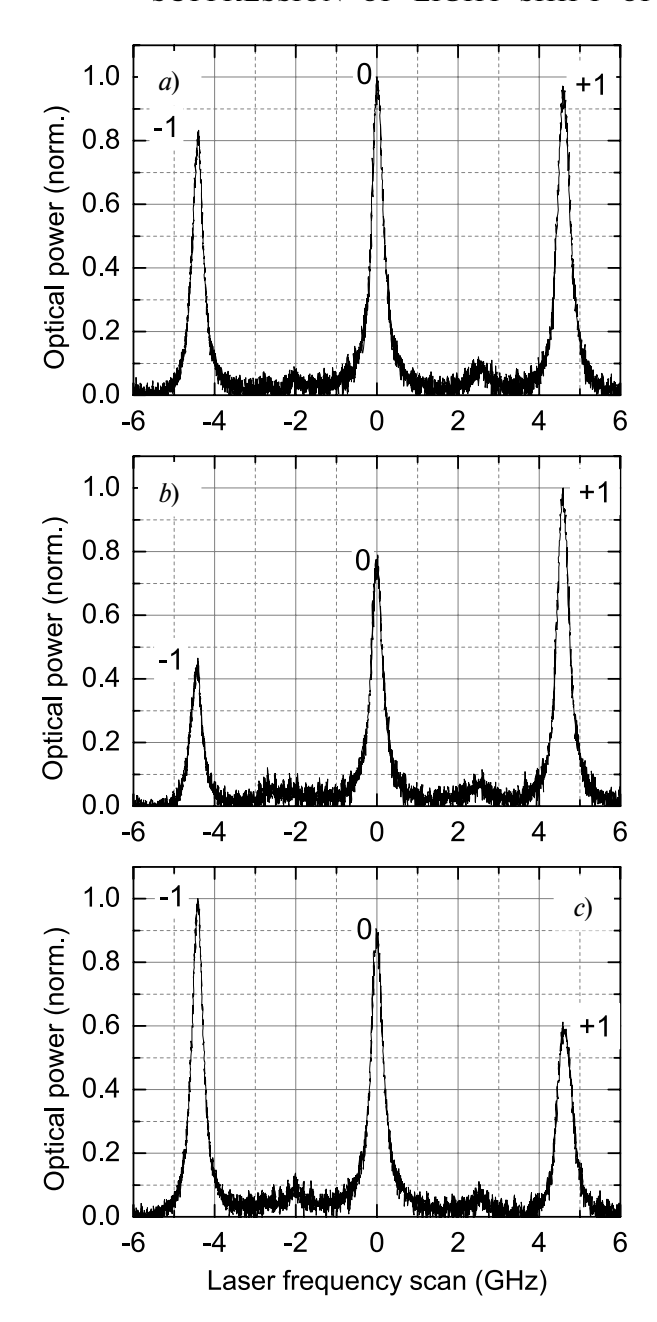


Fig. 4. Light shift of the error signal from the "0-0" transition frequency only when using microwave modulation of VCSEL current (a) and when using double modulation first of the laser current, then of radiation using EOM In the first case, the microwave splitter was not used (see Fig. 1), and in the second case, the specified microwave power was divided equally between VCSEL and EOM. The constant background, independent of P, has been subtracted from both figures.  $U_{FOM}\!\approx\!-3$  V.  $T\!\approx\!60^{\circ}\mathrm{C}$ 

the bias voltage on the EOM  $(U_{EOM})$ . When a monochromatic wave enters the EOM, this voltage allows efficient control of energy redistribution between the sidebands and the optical carrier frequency, and, in particular, allows complete suppression of the carrier, leaving only sidebands of  $\pm 1$  orders at the output. In our case  $U_{EOM}$  is used as another degree of freedom to control the radiation spectrum asymmetry. Moreover, this parameter is much more convenient than  $P_{\mu}$ , since microwave power often cannot be increased sufficiently to observe significant asymmetry. Specifically, with increasing  $P_{u}$ , VCSEL may exhibit multi-mode generation regime [26]. Thus, the VCSEL used in our experiments did not allow microwave power above approximately 1.5 mW, i.e., it cannot achieve



**Fig. 5.** Spectra of VCSEL radiation passed through EOM at  $U_{EOM} = -2 \text{ V } (a), \ U_{EOM} = -1 \text{ V } (b) \ \text{and} \ U_{EOM} = -3.5 \text{ V } (c).$  The total power of the microwave signal before the splitter (see Fig. 1) is approximately 1.2 mW (1 dBm)

sufficiently high frequency modulation indices to observe the dependence  $\Delta_f(P)$  as a horizontal straight line in Fig. 4 a, when the Stark shift of the error signal becomes zero (see, for example, [25, 32]).

Unlike  $P_{\mu}$ , parameter  $U_{EOM}$  allows for more flexible control of the radiation spectrum asymmetry, distributing more optical power either to the +1, order band or to the -1, order band, as shown in Fig. 5. Indeed, Fig. 5a shows that at

 $U_{EOM}$  = -2 V the radiation spectrum has relatively small asymmetry, similar to the case of microwave modulation of the VCL current only (see Fig. 3). In this case, the optical powers of the sidebands differ by approximately 15%. In Fig. 5*b* this difference is much more significant and amounts to about 50%, with the highest power falling on the +1 order band. In Fig. 5*c* the situation is reversed: the -1 order band has the highest power.

Ultimately, by selecting a combination of values  $P_{\mu}$  and  $U_{EOM}$  one can achieve significantly nonlinear behavior of the function  $\Delta_f(P)$ , as shown in Fig. 4 b. For example, the figure shows that at  $P_{\mu} \approx 1.2$  mW and  $U_{EOM} \approx -3$  V in dependence  $\Delta_f(P)$  there is a gentle minimum (red triangles). The position of this minimum sets the optimal optical power  $P_{opt} \approx 8$   $\mu$ W, at which the CPT frequency will be weakly sensitive to small variations in total optical power in the cell. Note that such optimum is also present for smaller values of  $P_{\mu}$ .

The spectrum asymmetry and, consequently, the position of the optimum in Fig. 4 *b* can also be controlled using the relative phase between amplitude and frequency types of spectrum modulation. In our experiment, this could be accomplished by adjusting the length of wires connecting the splitter to the microwave generator (see Fig. 1). This can be implemented more precisely using appropriate electronics (phase shifter for the microwave signal).

## 3. CONCLUSIONS

In this work, a new method for compensating the light shift frequency of OFS based on CPT resonances was investigated. This method involves using double microwave modulation: the pump current of the DFB laser and the intensity of laser radiation passing through the amplitude EOM are modulated at the same microwave frequency. It was experimentally shown that this method allows for more flexible control of the emission spectrum asymmetry compared to using only microwave modulation of the laser current, as in modern miniature atomic clocks based on CPT. Ultimately, the use of double frequency and amplitude modulation made it possible to observe a nonlinear dependence of the  $\Delta_f$  error signal shift on the total optical power P, which contains an extremum. The position of this extremum sets the optimal optical

power, near which the QFS frequency has low sensitivity to small variations in the total optical power in the cell with atoms. On a qualitative level, such behavior  $\Delta_f(P)$  agrees with the theory presented in [44], from which we conclude that the observed light shift dependence is related to the influence of CPT resonance asymmetry. Nevertheless, further development of the theory of the observed effect is necessary.

For direct measurement of long-term frequency stability (Allan deviation) using the proposed method of CPT resonance excitation, a cesium cell with a different buffer gas composition than the one used in our experiments (130 Torr neon) is required. For example, a specific mixture of Ar and Ne can be used to ensure insensitivity of the CPT resonance position to small temperature variations near  $60^{\circ}$ C. Based on data from [48], it can be shown that when using the cell at our disposal, this sensitivity is significant and amounts to about 9 Hz/K. Such temperature sensitivity of the frequency shift will lead to relative long-term QFS instability at the level of about  $2 \cdot 10^{-12}$ .

After suppressing the temperature shift effect through the correct ratio of buffer gases in the cell, light shifts will be the main contributors to long-term instability. Based on the results presented in our work, it follows that controlling the optical power at the level of 1% from the optimal power (near the extremum of dependence  $\Delta_f(P)$ , see Fig. 3b) will lead to a relative frequency shift at the level of  $5 \cdot 10^{-13}$ . Thus, when using the proposed method of double frequency and amplitude modulation of radiation, the long-term frequency instability of the QFS caused by small optical power drift can be several times lower than demonstrated by advanced samples of miniature QFS/CPT [8,9].

### **FUNDING**

This work was supported by the Russian Science Foundation (grant No. 22-12-00279).

#### **REFERENCES**

- 1. T. N. Bandi, N. M. Desai, J. Kaintura et al., GPS Solutions **26**, 54 (2022).
- 2. E. Fernández, D. Calero, and M. Eulàlia Parés, Sensors 17, 370 (2017).

- 3. S. Nydam, J. Anderson, N. S. Barnwell et al., *A Compact Optical Time Transfer Instrument for Ground-to-Space Synchronization of Clocks*, in Proc. AIAA SPACE and Astronautics Forum and Exposition, Orlando, Florida, USA, 12-14 September 2017. P. 5381.
- **4.** B. L. Schmittberger Marlow and D. R. Scherer, IEEE Trans. UFFC **68**, 2007 (2021).
- 5. S. E. Freeman, L. Emokpae, J. S. Rogers, and G. F. Edelmann, J. Acoust. Soc. Am. **143**, EL74 (2018).
- C. L. Chow, Y, Zhang, M. S.Tse et al., Overview of Project SPATIUM – Space Precision Atomicclock TIming Utility Mission, in Proc. 33rd Annual AIAA/ USU Conference on Small Satellites, Logan, Utah, USA, 3-8 August 2019. Report no. SSC19-WKVII-07.
- 7. J. Kitching, Appl. Phys. Rev. 5, 031302 (2018).
- H. Zhang, H. Herdian, A. T. Narayanan et al., IEEE J. Solid-St. Circ. 54, 3135 (2019).
- **9.** M. N. Skvortsov, S. M. Ignatovich, V. I. Vishnyakov et al., Quantum Electronics **50**, 576 (2020).
- **10**. E. Batori, C. Affolderbach, M. Pellaton et al., Phys. Rev. Applied **18**, 054039 (2022).
- **11**. Z. L. Newman, V. Maurice, T. Drake et al., Optica **6**, 680 (2019).
- **12**. D. Brazhnikov, M. Petersen, G. Coget et al., Phys. Rev. A **99**, 062508 (2019).
- **13**. A. Sargsyan, A. Amiryan, Y. Pashayan-Leroy et al., Opt. Lett. **44**, 5533 (2019).
- **14**. V. Maurice, Z. Newman, S. Dickerson et al., Opt. Express **28**, 24708 (2020).
- **15**. D. V. Brazhnikov, S. M. Ignatovich, I. S. Mesenzova et al., Quantum Electronics **50**, 1015 (2020).
- **16**. A. Gusching, M. Petersen, N. Passilly et al., J. Opt. Soc. Am. B **38**, 3254 (2021).
- **17**. D. V. Brazhnikov, S. M. Ignatovich, I. S. Mesenzova et al., J. Phys. Conf. Ser. **1859**, 012019 (2021).
- **18**. A. M. Mikhailov, R. Boudot, and D. V. Brazhnikov, JETP **160**, 818 (2021) [A. M. Mikhailov, R. Boudot, and D. V. Brazhnikov, JETP **133**, 696 (2021)].
- **19**. F. Riehle, *Frequency Standards: Basics and Applications*, Wiley-VCH Verlag GmbH & Co. KGaA, Weinheim (2004).
- **20**. F. Levi, A. Godone, and J. Vanier, IEEE Trans. UFFC **47**, 466 (2000).
- **21**. D. S. Chuchelov, V. V. Vassiliev, M. I. Vaskovskaya et al., Phys. Scripta **93**, 114002 (2018).
- **22**. D. Miletic, C. Affolderbach, M. Hasegawa et al., Appl. Phys. B **109**, 89 (2012).
- **23**. M. I. Vaskovskaya, E. A. Tsygankov, D. S. Chuchelov et al., Opt. Express **27**, 35856 (2019).

- 24. D. V. Brazhnikov, S. M. Ignatovich, and M. N. Skvortsov, Phys. Rev. Appl. 21, 054046 (2024)
- . Y. Yin, Y. Tian, Y. Wang, and S. Gu, Spectrosc. Lett. **50**, 227 (2017).
- . A. O. Makarov, S. M. Ignatovich, V. I. Vishnyakov et al., AIP Conf. Proc. **2098**, 020010 (2019).
- . V. I. Yudin, M. Yu. Basalaev, A. V. Taichenachev et al., Phys. Rev. Appl. **14**, 024001 (2020).
- . M. Abdel Hafiz, R. Vicarini, N. Passilly et al., Phys. Rev. Appl. **14**, 034015 (2020).
- . K. A. Barantsev and A. N. Litvinov, J. Opt. Soc. Am. B **39**, 230 (2022).
- . C. Carlé, M. Abdel Hafiz, S. Keshavarzi et al., Opt. Express **31**, 8160 (2023).
- . D. A. Radnatarov, S. M. Kobtsev, V. A. Andryushkov et al., JETP Lett. **117**, 504 (2023).
- . D. Radnatarov, S. Kobtsev, V. Andryushkov, and T. Steschenko, Proc. SPIE **11817**, 1181700 (2021).
- . A. P. Bogatov, A. E. Drakin, M. I. Vaskovskaya et al., Opt. Lett. **47**, 6425 (2022)
- . K. N. Savinov, A. K. Dmitriev, and A. V. Krivetskii, Quantum Electronics **52**, 116 (2022).
- . C. Affolderbach, C. Andreeva, S. Cartaleva et al., Appl. Phys. B **80**, 841 (2005).

- . C. Long and K. Choquette, J. Appl. Phys. **103**, 033101 (2008).
- . F. Gruet, A. Al-Samaneh, E. Kroemer et al., Opt. Express **21**, 5781 (2013).
- . E. A. Tsygankov, S. A. Zibrov, M. I. Vaskovskaya et al., Opt. Express **30**, 2748 (2022).
- . K. Deng, T. Guo, J. Su et al., Phys. Lett. A **373**, 1130 (2009).
- . M. Merimaa, T. Lindvall, I. Tittonen, and E. Ikonen, J. Opt. Soc. Am. B **20**, 273 (2003).
- 41. E. D. Black, Am. J. Phys. 69, 79 (2001).
- . I. Ben-Aroya, M. Kahanov, and G. Eisenstein, Opt. Express **15**, 15060 (2007).
- . V. I. Yudin, A. V. Taichenachev, M. Yu. Basalaev, and D. V. Kovalenko, Opt. Express **25**, 2742 (2017).
- . V. I. Yudin, M. Yu. Basalaev, A. V. Taichenachev et al., Phys. Rev. A **108**, 013103 (2023).
- . N. Beverini, P. Minguzzi, and F. Strumia, Phys. Rev. A **4**, 550 (1971).
- . W. Happer, Rev. Mod. Phys. **44**, 169 (1972).
- . A. V. Taichenachev, V. I. Yudin, R. Wynands et al., Phys. Rev. A **67**, 033810 (2003).
- . O. Kozlova, S. Guérandel, and E. de Clercq, Phys. Rev. A **83**, 062714 (2011)